

Article

Chloride Binding Properties of a Macrocyclic Receptor Equipped with an Acetylide Gold(I) Complex: Synthesis, Characterization, Reactivity, and Cytotoxicity Studies

Andrea Rivoli ^{1,2}, Gemma Aragay ¹ , María Concepción Gimeno ³  and Pablo Ballester ^{1,4,*} 

¹ Institute of Chemical Research of Catalonia (ICIQ), The Barcelona Institute of Science and Technology (BIST), Av. Paisos Catalans 16, 43007 Tarragona, Spain; arivoli@iciq.es (A.R.); garagay@iciq.es (G.A.)

² Departament de Química Analítica i Química Orgànica, Universitat Rovira i Virgili (URV), c/Marcel·lí Domingo 1, 43007 Tarragona, Spain

³ Departamento de Química Inorgánica, Instituto de Síntesis Química y Catálisis Homogénea (ISQCH) CSIC-Universidad de Zaragoza, 50009 Zaragoza, Spain; gimeno@unizar.es

⁴ ICREA, Passeig Lluís Companys 23, 08010 Barcelona, Spain

* Correspondence: pballester@iciq.es

Abstract: In this work, we report the synthesis and characterization of a mono-nuclear “two wall” aryl-extended calix[4]pyrrole receptor (**2Au**) decorated with an acetylide-gold(I)-PTA complex at its upper rim. We describe the ¹H NMR titration experiments of **2Au** and its “two wall” aryl-extended calix[4]pyrrole synthetic precursors: the non-symmetric mono-iodo-mono-ethynyl **2** and the symmetric bis-iodo **3** with TBACl in dichloromethane and acetone solution. In acetone solution, we use isothermal titration calorimetry (ITC) experiments to thermodynamically characterize the formed 1:1 chloride complexes and perform pair-wise competitive binding experiments. In both solvents, we measured a decrease in the binding constant of the mono-nuclear **2Au** complex for chloride compared to the parent mono-iodo-mono-ethynyl **2**. In turn, receptor **2** also shows a reduction in binding affinity for chloride compared to its precursor bis-iodo calix[4]pyrrole **3**. The free energy differences (ΔG) of the 1:1 chloride complexes cannot be exclusively attributed to their dissimilar electrostatic surface potential values either at the center of the *meso*-phenyl wall or its *para*-substituent. We conclude that solvation/desolvation processes play an important role in the stabilization of the chloride complexes. In acetone solution and in the presence of TBACl, **6Au**, a reference compound for the acetylide Au(I)•PTA unit, produces a bis(alkynyl)gold(I) anionic complex [**7Au**][−]. Thus, the observation of two separate sets of signals for the bound aromatic calix[4]pyrrole protons, when more than 1 equiv. of the salt is added, is assigned to the formation of the chloride complexes of **2Au** and of the “in situ” formed calix[4]pyrrole anionic dimer [**8Au**][−]. Finally, preliminary data obtained in cell viability assays of **2Au** and **6Au** with human cancer cells lines assign them with moderate activities showing that the calix[4]pyrrole unit is not relevant.

Keywords: calix[4]pyrrole; anion receptors; acetylide gold(I) complexes; cytotoxicity studies



Citation: Rivoli, A.; Aragay, G.; Gimeno, M.C.; Ballester, P. Chloride Binding Properties of a Macrocyclic Receptor Equipped with an Acetylide Gold(I) Complex: Synthesis, Characterization, Reactivity, and Cytotoxicity Studies. *Inorganics* **2022**, *10*, 95. <https://doi.org/10.3390/inorganics10070095>

Academic Editors: Rainer Winter and Bruno Therrien

Received: 23 June 2022

Accepted: 2 July 2022

Published: 5 July 2022

Publisher's Note: MDPI stays neutral with regard to jurisdictional claims in published maps and institutional affiliations.



Copyright: © 2022 by the authors. Licensee MDPI, Basel, Switzerland. This article is an open access article distributed under the terms and conditions of the Creative Commons Attribution (CC BY) license (<https://creativecommons.org/licenses/by/4.0/>).

1. Introduction

Alkynyl gold(I) complexes are important elements in the construction of molecular receptors and metal ligands [1,2]. Notably, arylacetylide gold(I) units have interesting emissive properties deriving from the intraligand ³($\pi\pi^*$) state owing to the introduction of spin-orbit coupling with the heavy metal. In this vein, the Yam's group decorated calix[4]arene scaffolds with arylalkynyl gold(I) complexes to produce multi-nuclear luminescent probes suitable for cation binding [3–5]. In these constructs, the observed emission changes were also assigned to modulations of the existent Au(I)⋯Au(I) aurophilic interactions upon cation binding. Mono-nuclear arylacetylide gold(I) complexes were incorporated to simple hydrogen-bonding donor functional groups, i.e., urea and amide, obtaining chemosensors

capable of selective anion binding [6,7]. Calix[4]pyrroles are macrocyclic hosts displaying interesting properties for the selective and high affinity binding of anions, ion-pairs, and electron-rich substrates through hydrogen-bonding interactions [8–10]. Examples of the incorporation of metal centers in the calix[4]pyrrole scaffold are scarce in the literature. Cafeo et al. described the incorporation of a Pt(II) metal center by *trans*-coordination with the amino group at the upper rim of the “mono wall” *meso-p*-aminophenyl-calix[4]pyrrole [11]. Using *in vitro* studies with different cancer cell lines, the authors demonstrated that the cytotoxic activity of the compounds derived from the co-existence of the calix[4]pyrrole element and the bound Pt(II) metal center. Recently, we described the synthesis and characterization of the anion receptor **1Au** based on a mono-nuclear gold(I) acetylide complex containing a “two wall” calix[4]pyrrole as recognition element for anions [12]. We installed the acetylide gold(I) complex as *para*-substituent of one of the *meso*-aryl groups of the “two wall” aryl extended calix[4]pyrrole **1Au**. We used 1,3,5-triaza-7-phosphaadamantane (PTA) as ancillary ligand to stabilize the acetylide gold(I) complex. Compared to the 10 α ,20 α -bis-*p*-ethynylaryl-calix[4]pyrrole parent compound **1** that did not show any emission properties, the mono-nuclear gold(I) derivative **1Au** displayed weak emission upon excitation at 300 nm. We measured a five-fold decrease in the binding affinity of chloride for the mono-nuclear gold(I) calix[4]pyrrole derivative **1Au** compared to its parent di-alkynyl **1** in dichloromethane solution. We assigned this difference to the existence of repulsive chloride– π interactions between the *meso*-phenyl group decorated with the *para*-acetylide gold(I) and the bound anion. During the ^1H NMR titrations, we detected two separate sets of signals for the aromatic protons of the bound calix[4]pyrrole in the $\text{Cl}^- \bullet \mathbf{1Au}$ complex. One set of signals had a significantly lower intensity than the other. We hypothesized that receptor **1Au** coordinated the chloride by adopting cone and partial-cone conformations (Figure 1) [13,14]. Surprisingly to us, the two putative isomers of the $\text{Cl}^- \bullet \mathbf{1Au}$ complex were involved in a chemical exchange process featuring slow dynamics on the chemical shift time scale. We decided to undertake the current work in order to evaluate the generalization of the above observations. We also wanted to verify that the low-intensity set of proton signals observed in the titration of **1Au** with TBACl was not caused by its transformation into a new species induced by the addition of the salt in excess.

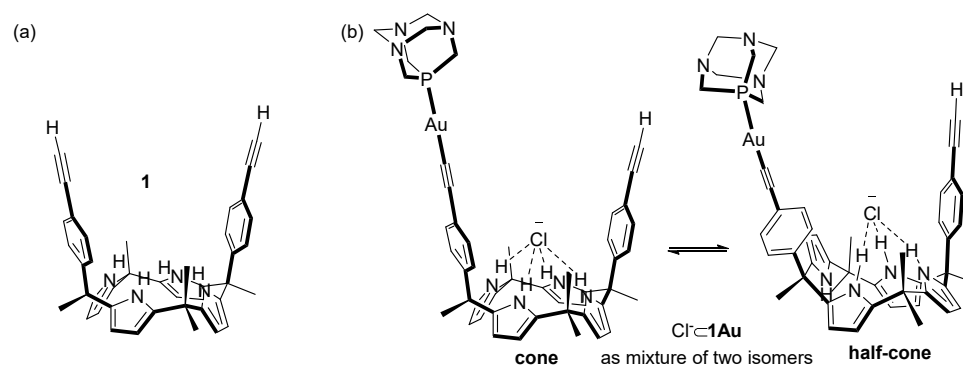
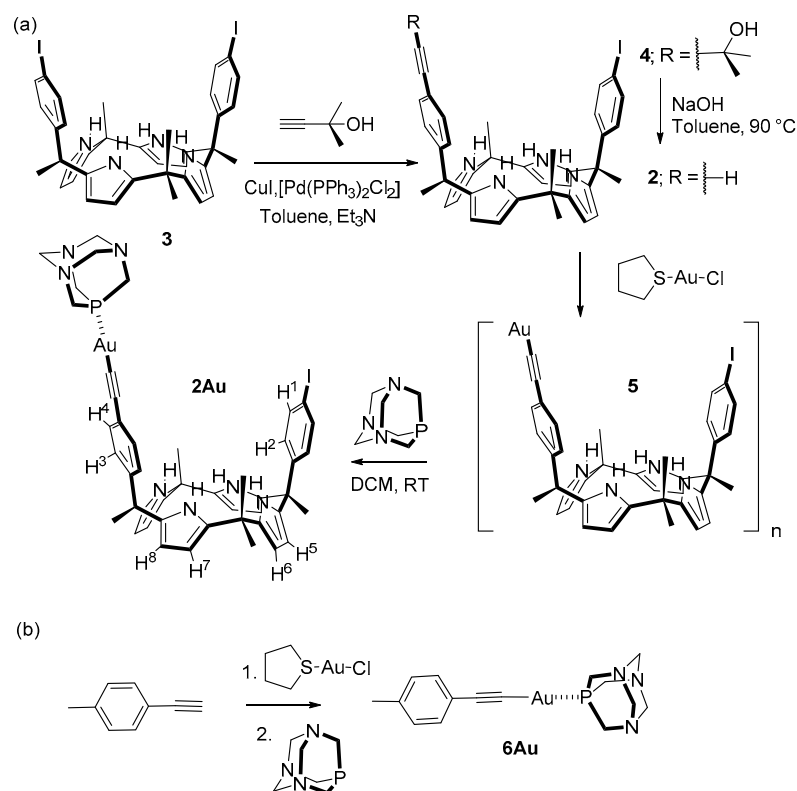


Figure 1. (a) Line-drawing structure of the bis-alkynyl calix[4]pyrrole **1**; (b) equilibrium between the two putative conformers of the 1:1 complexes of the mono-nuclear calix[4]pyrrole receptor **1Au** with chloride, $\text{Cl}^- \bullet \mathbf{1Au}$, hypothesized in our previous work [12].

Herein, we report the synthesis and characterization of a mono-nuclear gold(I) calix[4]pyrrole receptor **2Au** (Scheme 1), analogue to **1Au**. We also describe the results of the ^1H NMR titration experiments of receptor **2Au** and its synthetic precursors, **2** and **3**, with TBACl in dichloromethane and acetone solution. We perform ITC experiments and pair-wise competitive experiments for the accurate thermodynamic characterization of the 1:1 chloride complexes formed in acetone solution. We measured a decrease in the binding stability of the 1:1 complex of **2Au** with chloride compared to the parent *meso*-10 α ,20 α -*p*-ethynylphenyl-*p*-iodophenyl receptor **2**, and the C_{2v} symmetrical *p*-iodophenyl precursor **3**. We performed

DFT calculations and computed the ESP values at the center of the aromatic ring and at the *para*-substituent to support the trend in binding affinities experimentally measured.



Scheme 1. Synthetic schemes for the preparation of (a) the calix[4]pyrrole mono-nuclear gold(I) acetylide complex **2Au** and (b) the reference mono-nuclear gold(I) acetylide **6Au**.

In analogy to the observations previously made for **1Au** [12], the titrations of **2Au** with incremental amounts of TBACl, either in dichloromethane-*d*₂ or acetone-*d*₆ solutions, produced the appearance of two separate sets of aromatic signals for the bound receptor. Previously, we ascribed the two sets of signals to existence of the “bound” receptor as a mixture of two conformers (Figure 1b). The reference compound **6Au**, lacking the calix[4]pyrrole unit, evidenced the lability of acetylide-Au(I)-PTA unit in the presence of chloride. We concluded that **1Au**/**2Au** bind chloride exclusively in the cone conformation and that the presence of free chloride in solution induced the formation of a gold(I)-anionic calix[4]pyrrole dimer [**8Au**][−]. We briefly describe the cytotoxic properties of **2Au** and the reference compound **6Au** using different human cancer cell lines.

2. Results and Discussion

2.1. Synthesis

The mono-nuclear acetylide gold(I) complex **2Au** possesses a *para*-iodo substituent in the non-metalated *meso*-phenyl instead of the *para*-ethynyl present in **1Au**. This structural modification was expected to increase the stability of **2Au** and facilitate its synthesis. Compound **2Au** contains an α,α -“two wall” calix[4]pyrrole binding site and is prepared in four synthetic steps from the well-known *meso*-hexamethyl-10*α*,20*α*-bis-*p*-iodophenyl-calix[4]pyrrole **3** (Scheme 1a) [15]. Firstly, following described synthetic methodology [15,16], the statistical Sonogashira reaction of the C_{2v} symmetric bis-iodo **3** with 2-methyl-3-butyn-2-ol (5 equiv.), at r.t in dry toluene and triethylamine amine as base, allowed the isolation of the unprecedented mono-substituted iodo-ethynyl protected calix[4]pyrrole **4**. Compound **4** was obtained in 33% yield after column chromatography purification of the reaction crude. Next, the treatment of **4** with sodium hydroxide in toluene at 90 °C for 12 h yielded the mono-iodo-mono-ethynyl calix[4]pyrrole **2** in 70%

yield following a simple reaction work-up [15,16]. We treated mono-iodo-mono-ethynyl **2** with freshly prepared chloro(tetrahydrothiophene)gold(I) [17], (tht)AuCl, to obtain the corresponding oligomeric gold(I) acetylide **5**, probably having both σ and π bonds to the alkynyl group. Compound **5** was used immediately and without further purification. Finally, **5** was reacted with 1,3,5-triaza-7-phosphaadamantane (PTA) [18] to yield the mono-nuclear gold(I) complex **2Au** in 40% yield, through the replacement of the gold–alkyne bonds with the stronger phosphine donor [19]. All compounds, except **5**, were fully characterized by a complete set of high-resolution spectra (see SI). Using the synthetic strategy employed for the conversion of **2** into **2Au**, we prepared the mono-nuclear gold(I) acetylide complex **6Au** starting from *p*-ethynyl-toluene (Scheme 1b). **6Au** was used as a reference compound to investigate the stability of the phenyl-ethynyl- Au(I)•PTA unit of **2Au** upon incremental additions of TBACl.

2.2. Binding Studies of “Two Wall” Calix[4]Pyrrole Receptors **2**, **3**, and **2Au** with TBACl. Study of the Upper Rim Substituent Effect on Chloride Binding

2.2.1. Dichloromethane Solution

We probed the interaction of the mono-nuclear calix[4]pyrrole **2Au** with chloride in dichloromethane- d_2 solution using ^1H NMR spectroscopy. We used tetrabutylammonium chloride (TBACl) as chloride precursor. In agreement with a C_s symmetry, the ^1H NMR spectrum of **2Au** displayed four doublets for its aromatic protons, four overlapping double doublets for the β -pyrrole protons and four singlets for its methyl groups. The two pairs of diastereotopic pyrrole NHs resonated as a broad singlet centered at $\delta = 7.3$ ppm (Figure 2a).

The incremental addition of TBACl to the 1.9 mM solution of **2Au** produced noticeable chemical shift changes in most proton signals of the mono-nuclear receptor. In particular, all aromatic doublets shifted upfield, signifying the existence of chloride– π interactions [20]. The doublets of the β -pyrrole protons moved in opposite direction in response to the conformational change experienced by the receptor. That is, from alternate in the free state to cone in the bound counterpart. In the presence of ~ 20 equiv. of TBACl, the pyrrole NHs were visible in the downfield region of the spectrum as a broadened signal centered at $\delta = 9.7$ ppm. This signal shifted even further downfield as the concentration of the salt was increased from 20 to 27 equiv. (Figure 2e,f). The downfield shifts experienced by the NH protons indicated their involvement in hydrogen bonding interactions with the bound chloride. In fact, it is well known, that “two wall” calix[4]pyrroles bind the chloride anion by establishing four convergent hydrogen-bonds with the pyrrole NHs [20]. Notably, in the initial phase of the titration, the multiplet assigned to the methylene protons alpha to the nitrogen atom of the TBA^+ cation (Figure 2, aliphatic region) appeared upfield shifted with respect to the same protons in the free TBACl salt. However, as the concentration of the TBACl increased the triplet moved downfield towards the chemical shift value of free TBACl. In chlorinated non-polar solvents like dichloromethane- d_2 , ion-pairs, like TBACl, are not significantly dissociated. Likewise, the interaction of TBACl with the mono-nuclear calix[4]pyrrole **2Au** is expected to produce an ion-paired complex. The initial upfield shifts observed for the TBA^+ alpha methylene protons, located the TBA^+ cation of the 1:1:1 ion-paired complex, $\text{Cl}^- \bullet 2\text{Au} \bullet \text{TBA}^+$, in the shallow and electron rich cavity defined by the pyrrole rings of the receptor’s cone conformation. This cavity is opposite to the binding site of the chloride resulting in a receptor-separated binding geometry for the ion paired complex, $\text{Cl}^- \bullet 2\text{Au} \bullet \text{TBA}^+$ [10,21,22]. During the titration, the overall concentration of TBACl is increased favoring the relative amount of free salt. Because the TBA^+ cation of the free salt is involved in a chemical exchange equilibrium with the bound counterpart displaying fast dynamics on the chemical shift timescale, the increase of the relative concentration of the free TBACl provokes that the alpha methylene proton signal move downfield, approaching the chemical shift value of the free salt.

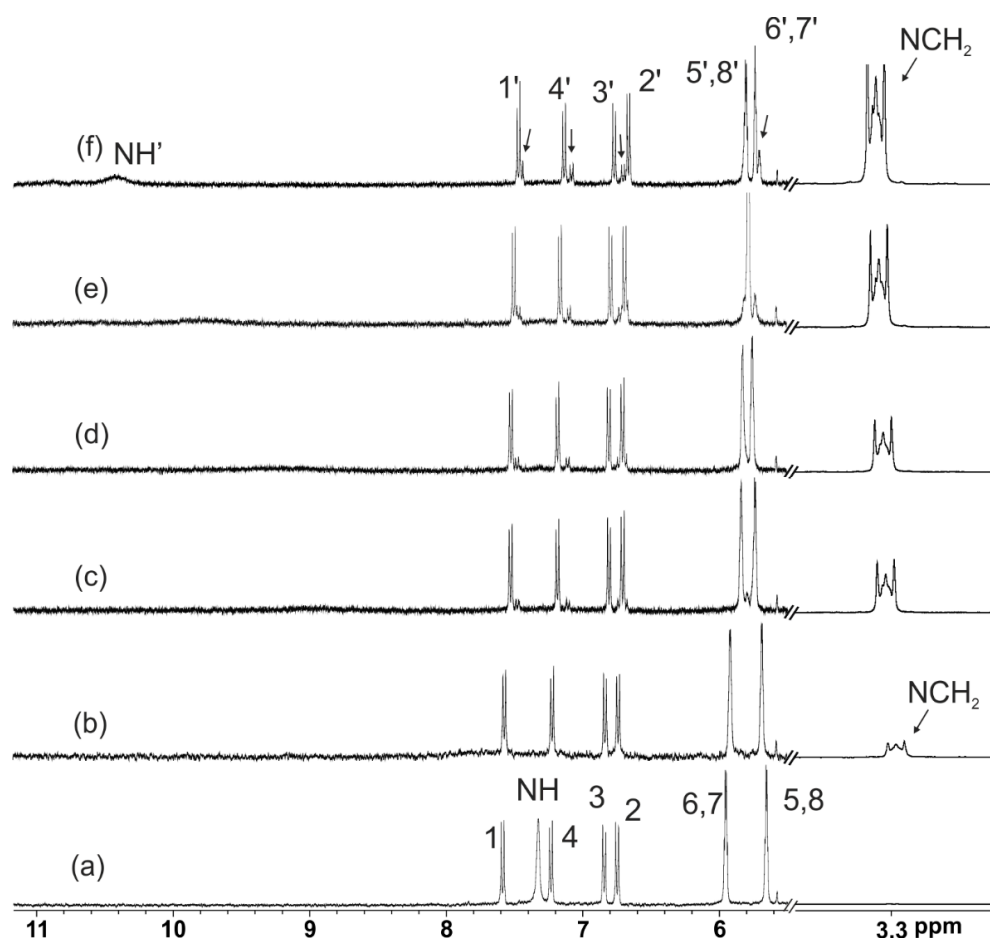


Figure 2. Selected downfield and upfield regions (aromatic and TBA regions, respectively) of the ^1H NMR spectra (400 MHz, CD_2Cl_2 , 298 K) acquired during the titration of the mono-nuclear **2Au** calix[4]pyrrole receptor ($[\mathbf{2Au}] = 1.9$ mM) with TBACl: (a) 0 (b) 1 (c) 4.5 (d) 10.5 (e) 21 and (f) 27 equiv. added. See Scheme 1a for proton assignment. The scale of the aromatic region is increased 16 times with respect to the upfield TBA region in order to show the presence of the second set of aromatic proton signals.

We performed analogous titrations of the synthetic precursors of the mono-nuclear calix[4]pyrrole **2Au**, bis-iodo **3** and the mono-iodo-mono-ethynyl parent **2** obtaining very similar results. The most relevant difference between the three titrations was the appearance of a second set of aromatic signals in the case of **2Au**. This second set of signals had a reduced intensity and was initially detected when 4.5 equiv. of TBACl were added. The two sets of aromatic signals moved upfield as the concentration of TBACl was increased. The intensity of the second set of signals was also slightly increased upon the incremental addition of TBACl.

The chemical shift changes experienced by selected proton signals [23] of the calix[4]pyrroles **2Au**, **2**, and **3**, and the TBA^+ cation during the titrations were mathematically analyzed (non-linear regression) using the HypNMR2008 [24,25] software version 4.0.66, Leeds, England, UK and a 1:1 binding theoretical model. The fit of the data was good ($\sigma < 2.8$), supporting the formation of the 1:1:1 ion-paired ternary complex. The determined apparent binding constants are summarized in Table 1.

From the data listed in Table 1, we draw the following conclusions: (a) the substitution of one *p*-iodo substituent by one *p*-gold(I)acetylide in the scaffold of a “two wall” calix[4]pyrrole receptor (i.e., **3** vs. **2Au**) produced a drop in binding energy for TBACl of 0.71 kcal/mol; (b) the drop in binding affinity can be dissected into 0.49 kcal/mol produced by the substitution of the iodo group by the ethynyl counterpart (i.e., **3** vs. **2**) and the

0.22 Kcal/mol caused by the incorporation of a gold(I) phosphine moiety (i.e., **2** vs. **2Au**). Notably, these structural modifications are associated with changes in the electron surface potential (ESP) values of the *meso*-substituent. We used *p*-iodotoluene, *p*-ethynyltoluene and *p*-gold(I)acetylidetoene as model systems of the *meso*-phenyl substituent in **3**, **2** and **2Au**, respectively, to compute the ESP values at the center of the phenyl ring and at the *para*-substituent (ESP₁; ESP₂). Although the larger change in ESP values was caused by the introduction of the gold(I) phosphine moiety, **2** (−14.8; −18.7) vs. **2Au** (−30.3; −41.1), it did not translate into the most significant component of the dissected reduction of binding affinity (only 0.22 Kcal/mol of the total 0.71 Kcal/mol). Conversely, the substitution of the *p*-iodo substituent by the *p*-ethynyl counterpart having a reduced impact on ESP values (−13.1; −13.7 Kcal/mol for **3** vs. −14.8; −18.7 Kcal/mol for **2**) contributed more significantly in the energy difference of the corresponding chloride complexes (0.49 Kcal/mol). Taken together, these results indicated that the increase in electrostatic repulsive chloride− π interactions of the “two wall” calix[4]pyrrole complexes caused by the change of the *para*-substituent of one of the “walls” is not enough to explain the differences in complexes’ binding affinities measured experimentally. We concluded that solvation/desolvation processes are also important in accounting for these differences.

Table 1. Apparent binding constants (K_a , M^{−1}) of the ion-paired complexes of receptors **2**, **3**, and **2Au** with TBACl in dichloromethane. The value of the binding constants ratio using $K(\text{TBA}\bullet\mathbf{3}\bullet\text{Cl}^-)$ as reference and the corresponding $\Delta\Delta G$ are also listed. ESP values at the center of the phenyl ring and at the *para*-substituent (ESP₁; ESP₂) are indicated.

Receptor	$K_a \times 10^{-2}$ CD ₂ Cl ₂ ^a	$K(\text{TBA}\bullet\mathbf{3}\bullet\text{Cl}^-)$ / $K(\text{TBA}\bullet\mathbf{n}\bullet\text{Cl}^-)$	$\Delta\Delta G$ kcal/mol	ESP (Ar;Subst) kcal/mol ^b
Bis-iodo 3	2.54 ± 0.1	1	0	−13.1; −13.7
Mono-iodo-mono-ethynyl 2	1.11 ± 0.02	2.28 ± 0.10	0.49 ± 0.03	−14.8; −18.7
Mono-nuclear 2Au	0.76 ± 0.1	3.3 ± 0.14	0.71 ± 0.03	−30.3; −41.1

^a The titration experiments were performed in dichloromethane-*d*₂ solution at 298 K and monitored using ¹H NMR spectroscopy. The titration data were fit to a 1:1 theoretical binding model. ^b The reported values correspond to the center of the phenyl group and the center of the *para*-substituent, respectively, in the used model systems (see text for details).

2.2.2. Acetone Solution

Aiming at studying the differences in chloride binding energies for the series of “two wall” calix[4]pyrroles in a more polar solvent, we switched to acetone. In our previous study with the mono-nuclear **1Au**, we observed two sets of aromatic proton signals in the ¹H NMR spectra of the titration with TBACl in acetone-*d*₆ solution which were attributed to a mixture of two conformers in solution. Due to the polar nature of acetone, ion-pair salts are significantly dissociated. The TBA⁺ cation is well-solvated by acetone molecules. In contrast, the reduced solvation of the chloride anions provoked that the magnitude of the binding constant of the anionic calix[4]pyrrole complexes formed in acetone is larger than in dichloromethane. We monitored the interaction of receptor **2Au** with chloride using ¹H NMR spectroscopy and TBACl as anion precursor. The ¹H NMR spectra acquired during the titration of **2Au** with incremental amounts of TBACl in acetone-*d*₆ solution are depicted in Figure 3.

The incremental addition of TBACl produced the observation of two separate sets of broadened signals for the protons of **2Au**. This result is in contrast with the steady downfield/upfield shifts observed in dichloromethane-*d*₂. The observation of separate proton signals for the free and bound **2Au** indicated that the chemical exchange of the binding process displayed slow kinetics on the chemical shift timescale. The doublet emerging at $\delta = 11.4$ ppm was assigned to the hydrogen-bonded pyrrole NHs in the Cl[−]•**2Au** complex. All proton signals of bound **2Au** became sharp and well-defined in the presence of 1 equiv. of TBACl and did not experience changes when more salt was added. This result served to estimate the binding constant of the Cl[−]•**2Au** complex as larger than

10^4 M^{-1} . Throughout the titration, the signal of the methylene protons *alpha* to the nitrogen atom of the TBA⁺ cation did not experience chemical shift changes. This behavior supported the non-involvement of the TBA⁺ cation in the formation of the complex of chloride with **2Au** in this solvent, which as mentioned above existed mainly as anionic Cl⁻•**2Au** species. We also performed ¹H NMR titrations of **2** and **3** in acetone-*d*₆ with TBACl obtaining identical results. As mentioned above for the titrations in dichloromethane-*d*₂, only in the titration of **2Au** with TBACl in acetone-*d*₆ solution we observed two sets of signals with different intensity for the aromatic protons of the bound calix[4]pyrrole unit.

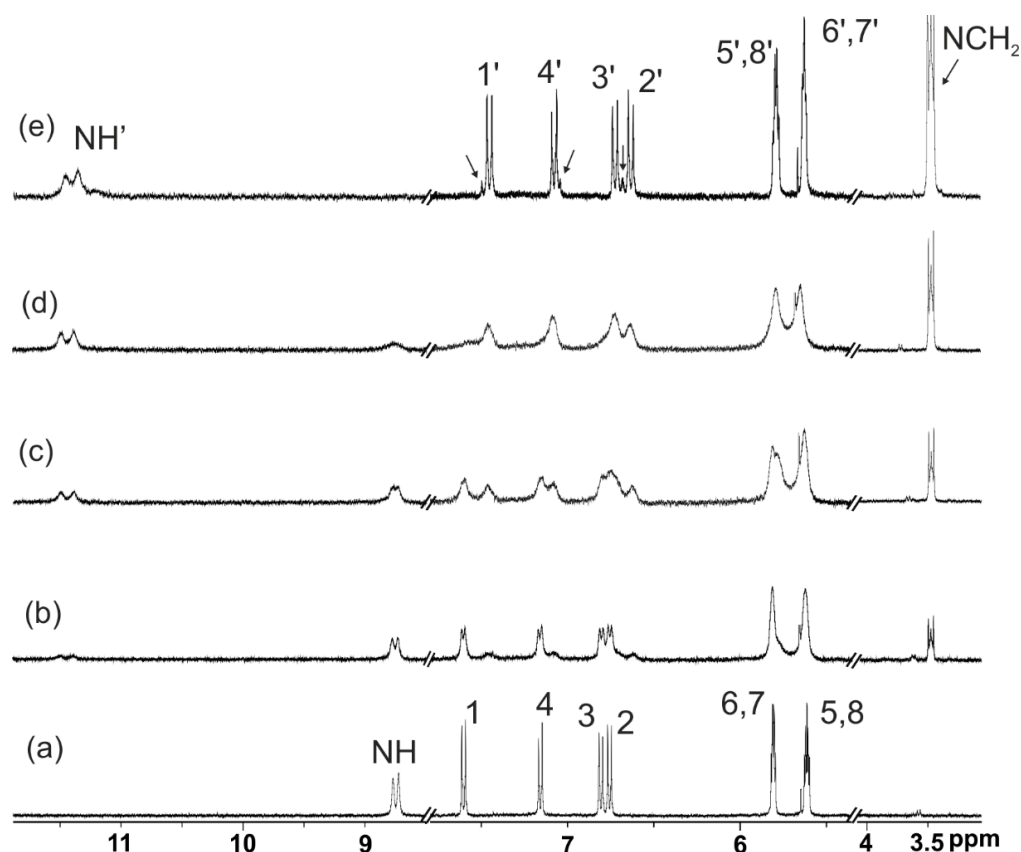


Figure 3. Selected regions of the ¹H NMR spectra (400 MHz, acetone-*d*₆, 298 K) acquired during the titration of receptor **2Au** (2.2 mM) with incremental amounts of TBACl: (a) 0 (b) 0.25 (c) 0.5 (d) 0.75 and (e) 1.2 equiv. Black arrows indicate the presence of a second set of proton signals.

Taken together, the obtained results showed that the used solvent impacted on the kinetics of the binding equilibrium of the calix[4]pyrroles with TBACl (fast in dichloromethane-*d*₂ and slow in acetone-*d*₆). However, in both solvents, the excess of TBACl produced the observation of two separate sets of signals for the aromatic protons of the calix[4]pyrrole. We raised some doubts on our previous assignment of the two sets of separate signals to the conformational isomers of the bound calix[4]pyrrole, cone and half-cone, in the ion-paired Cl⁻•**2Au**•TBA and anionic Cl⁻•**2Au** complexes (Figure 1b) [12]. In trying to settle the issue, we decided to investigate the effect caused by the addition of TBACl to an acetone solution of the model compound **6Au**. This compound lacking the calix[4]pyrrole unit was investigated as reference for the lability of the phenyl-ethynyl-Au(I)•PTA unit of **2Au** in the presence of chloride.

2.3. ¹H NMR Spectroscopy Analysis of the Addition of Incremental Amounts of TBACl to an Acetone Solution of **6Au**

The ¹H NMR spectrum of a 5 mM solution of **6Au** shows sharp and well-defined proton signals (Figure 4a). The addition of 2 equiv. of TBACl provoked the appearance of a

new set of signals for the aromatic protons and the methyl group (Figure 4b). The protons of the PTA ligand did not split; however, they experienced chemical shift changes. Notably, the intensity of the new set of signals increased with time at the expenses of those of **6Au** (Figure 4c). After several hours, the intensity changes reached a plateau. At this point, we added two additional equivalents of TBACl. The ^1H NMR spectrum of the mixture acquired immediately after the addition of the salt revealed that the new proton signals were the most intense ones (Figure 4d). At this stage, the increase in intensity of the new signals with time was not significant (Figure 4e). Nevertheless, incremental additions of TBACl caused further increased their intensity. It is worthy to note that we also observed the formation of a precipitate following each addition of TBACl. In the presence of 9 equiv. of TBACl and after several hours, the proton signals of the new species were almost exclusively observed in the ^1H NMR spectrum of the mixture (Figure S40). Taken together, these observations indicated that **6Au** reacted with TBACl to produce other species of unknown structure. We sought for precedents of this transformation in literature and found a report by Abu-Salah [26] describing the transformation of $p\text{-Ph}_3\text{P}\bullet\text{Au}(\text{I})\text{ethynyl-toluene}$ into the corresponding anionic bis-(alkynyl)gold(I) complex and $\text{Ph}_3\text{P}\bullet\text{Au}(\text{I})\text{-I}$ by addition of TBAI in acetone solution at r.t. Likewise, in the case at hand, the anionic bis-alkynyl-gold(I) complex $[\mathbf{7Au}]^-$ should be obtained from **6Au** by treatment with TBACl (Scheme 2). In any case, this is not the most common synthetic methodology used for the preparation of anionic bis-(alkynyl)gold(I) complexes. Using other synthetic methodologies, $[\mathbf{7Au}]^-$ and other bis-(alkynyl)gold(I) anionic complexes have already been reported in literature [27–29]. We compared the ^1H and ^{13}C NMR spectroscopic features of the new species in the reaction mixture of **6Au** with excess TBACl with those reported for compound $[\mathbf{7Au}]^-$. Based on the agreement of spectroscopic data, we concluded that the new species was indeed the anionic bis-(alkynyl)gold(I) complex $[\mathbf{7Au}]^-$. The ESI-MS spectrum of the solution showed an ion peak at m/z 427 with 10% relative intensity corresponding to $[\mathbf{7Au}]^-$ (Figure S43). The precipitate was also isolated and analyzed using ^1H and ^{31}P NMR spectroscopy. We observed the diagnostic signals for $\text{PTA}\bullet\text{Au}(\text{I})\text{-Cl}$ in the acquired NMR spectra. Finally, we performed a DOSY experiment of the acetone solution containing a mixture of **6Au**, $[\mathbf{7Au}]^-$, free PTA and partially solubilized $\text{PTA}\bullet\text{Au}(\text{I})\text{-Cl}$. As expected, the diffusion constant assigned to the signals related to $[\mathbf{7Au}]^-$ was smaller than that of any other species in solution (Figure S44). Moreover, the signals of the PTA ligand showed a larger diffusion constant suggesting that it was involved in other species with reduced hydrodynamic radii compared to $[\mathbf{7Au}]^-$ (i.e., free PTA and partially solubilized $\text{PTA}\bullet\text{Au}(\text{I})\text{-Cl}$) (see SI).

Based on the results obtained for the alkynyl gold(I) model compound **6Au** in the presence of chloride, we assigned the set of signals of low intensity observed in the ^1H NMR titrations of **2Au** with TBACl to the corresponding bis(alkynyl)gold(I)anionic dimer $[\mathbf{8Au}]^-$ (Scheme 2). The calix[4]pyrrole anionic dimer was formed to a reduced extent during the titration experiments because the amount of free chloride in solution was small. In fact, only when an excess of chloride was present in solution (>4.5 equiv. in dichloromethane- d_2 and >1.2 equiv. in acetone- d_6) we detected the signals of the anionic complex $[\mathbf{8Au}]^-$.

We also performed a DOSY experiment of a mixture of **2Au** containing a large excess of TBACl (i.e., 9 equiv.) in acetone- d_6 . The pseudo 2D plot of the DOSY (Figure S46) revealed that the two sets of signals related to the calix[4]pyrrole scaffold displayed different diffusion constants. The less intense set of signals, attributed to the chloride complex of the $[\mathbf{8Au}]^-$ dimer, displayed a smaller diffusion coefficient ($D = 9.4 \times 10^{-10} \text{ m}^2\cdot\text{s}^{-1}$) compared to the one assigned to the set of signals of 1:1 anionic $\text{Cl}^- \bullet \mathbf{2Au}$ complex ($D = 1.1 \times 10^{-9} \text{ m}^2\cdot\text{s}^{-1}$). This result is in agreement with the larger size of the chloride complex of the $[\mathbf{8Au}]^-$ dimer compared to that of the $\text{Cl}^- \bullet \mathbf{2Au}$ counterpart. The proton signals of the PTA ligand displayed a diffusion coefficient constant that did not coincide with any of the previous ones ($D = 1.6 \times 10^{-9} \text{ m}^2\cdot\text{s}^{-1}$). Most likely, the PTA is experiencing a chemical exchange that is fast on the DOSY timescale between different species present in solution (**2Au**, $\text{Cl}^- \bullet \mathbf{2Au}$, PTA, and partially solubilized $\text{PTA}\bullet\text{Au}(\text{I})\text{-Cl}$).

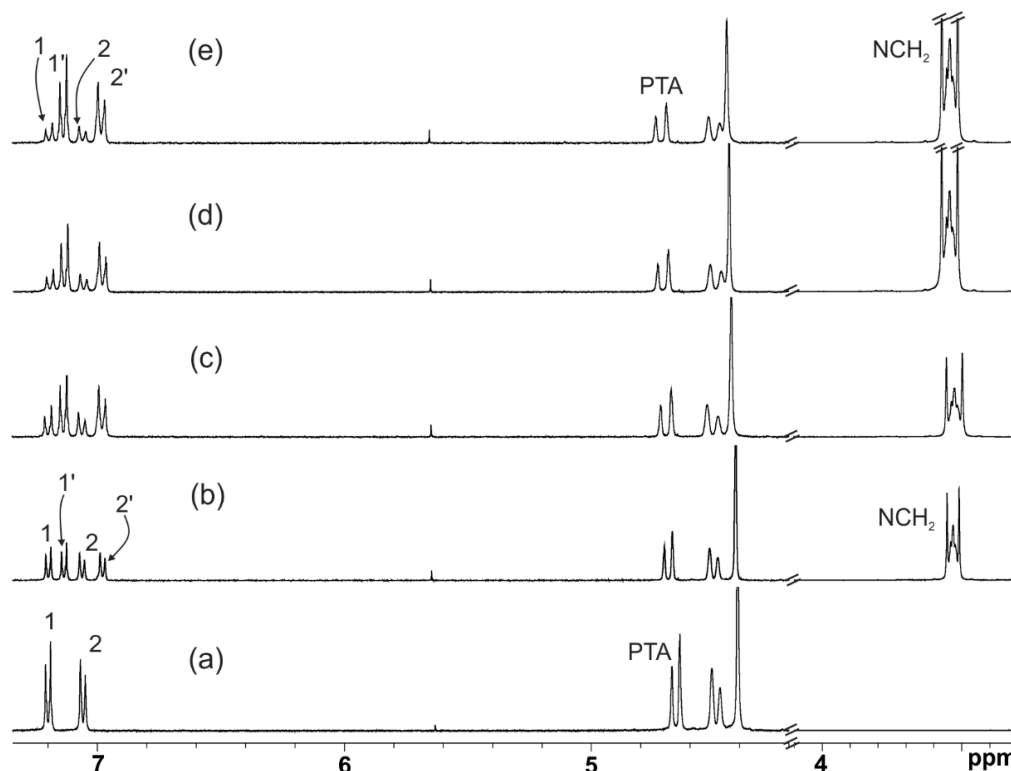
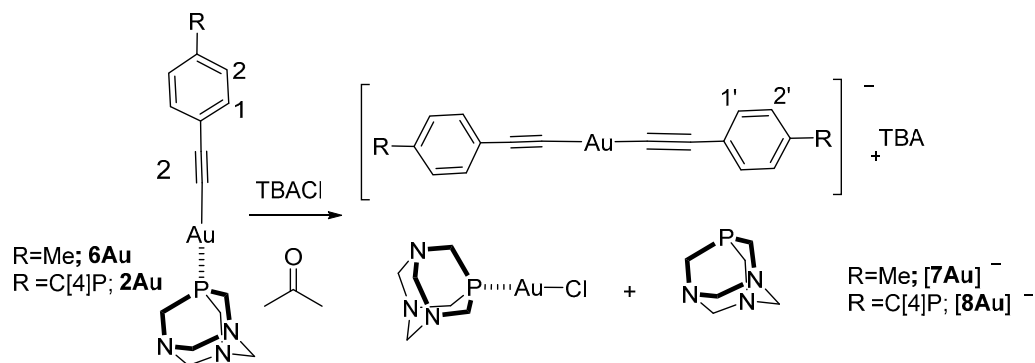


Figure 4. Selected regions of the ^1H NMR spectra (400 MHz, acetone- d_6 , 298 K) acquired during the titration of the model compound **6Au** (5 mM) (a) with incremental amounts of TBACl: (b) 2 equiv. of TBACl just after addition; (c) 2 equiv. of TBACl after 1.30 h; (d) 4 equiv. of TBACl just after addition (e) 4 equiv. of TBACl after 10 h. See Scheme 2 for proton assignment. Primed protons correspond to protons of $[\mathbf{7Au}]^-$ anionic dimer.



Scheme 2. Synthetic scheme for the formation of the anionic-bis(alkynyl)gold(I) complexes $[\mathbf{7Au}]^-$ and $[\mathbf{8Au}]^-$ with the corresponding proton assignment.

2.4. Isothermal Titration Calorimetry (ITC) Experiments

We considered that the accurate determination of the large binding constant values of receptor **2Au** and its synthetic precursors **2** and **3**, for chloride in acetone solution, required the use of isothermal titration calorimetry (ITC) experiments. In this type of experiments, the amount of free chloride in solution at the end of the titration is close to 1 equiv. For this reason, we expected that in the ITC experiments of **2Au**, the anionic dimer $[\mathbf{8Au}]^-$ would be formed to reduced extent. The computer-controlled injection of incremental amounts of TBACl, dissolved in acetone, to a solution of **2Au** in the same solvent ~ 10 -fold more diluted and placed in the calorimeter's cell produced the release of heat peaks. The binding isotherm obtained from the plot of the normalized integration of the heat peaks had the shape of a single sigmoidal curve with an inflexion point at a molar ratio

[TBACl]/[2Au] close to 1. This is the expected result for the formation of a 1:1 complex. The titration data beautifully fit the one set of sites model implemented in the Microcal ITC Data Analysis software, version 7.0, Northampton, MA, USA. The fitting procedure returned the values of the binding constant and the enthalpy of binding of the $\text{Cl}^- \bullet 2\text{Au}$ complex. We performed similar ITC experiments with receptors **2** and **3**. The determined thermodynamic constants (K_{app} , ΔH and $T\Delta S$) are summarized in Table 2. We refer to the binding constants as apparent owing to the simplification of the used binding model, which neither considers the association/dissociation of the ion-pairs (i.e., TBACl and TBACl•2Au) nor the contribution to the measured heat of the reaction yielding $[\mathbf{8Au}]^-$ and its putative binding to chloride. Notably, all binding processes are enthalpy and entropy favored. The large and favorable entropy term supports that solvation/desolvation processes are highly relevant in all binding processes. Surprisingly to us, the values of the free energy differences between the chloride complexes of 2Au and the calix[4]pyrrole receptors used as synthetic precursors, **2** and **3**, calculated in acetone are in reasonable agreement with those determined in dichloromethane solution for the ion-paired counterparts.

Table 2. Apparent binding constants (K_a , M^{-1}) and thermodynamic constants (Kcal mol^{-1}) of the binding equilibria of receptors **3**, **2**, and **2Au** with TBACl salt in acetone solution at 288 K determined by ITC experiments. The value of the binding constants ratio using $\text{K}(\text{TBA} \bullet \mathbf{3} \bullet \text{Cl}^-)$ as reference and the corresponding ΔG and $\Delta\Delta G$ are also listed.

	$K_a \times 10^{-4} (\text{M}^{-1})$ ($\text{CH}_3)_2\text{CO}^a$	ΔH	$-T\Delta S$	$\frac{\text{K}(\mathbf{3} \bullet \text{Cl}^-)}{\text{K}(\mathbf{n} \bullet \text{Cl}^-)}$	ΔG	$\Delta\Delta G$
Bis-iodo 3	15.1 ± 0.1	-3.70 ± 0.04	-3.13 ± 0.04	1.0	-6.83 ± 0.01	0.0
Mono-iodo-mono-ethynyl 2	9.2 ± 0.6	-3.29 ± 0.08	-3.25 ± 0.09	1.6 ± 0.1	-6.54 ± 0.04	0.29 ± 0.04
Mono-nuclear 2Au	5.5 ± 0.1	-2.83 ± 0.01	-3.43 ± 0.01	2.7 ± 0.1	-6.25 ± 0.01	0.58 ± 0.01

^a The titration data were fit to a 1:1 theoretical binding model.

2.5. Competitive Pair-Wise Binding Experiments

Owing to the side reaction produced by the addition of excess of TBACl to 2Au and the similarity of the magnitudes of the binding constants for chloride and the receptor series (2Au, 2, and 3) determined using ITC experiments, we decided to perform NMR pair-wise competitive binding experiments. The results of these experiments are expected to produce a better assessment of the ratios of the binding constant values. Moreover, in these experiments the TBACl is used in a sub-stoichiometric amount with respect to the competing calix[4]pyrroles (i.e., 1:2 molar ratio). These conditions warranted that the concentration of free chloride in solution is minimal during the experiment limiting the transformation of 2Au into the bis(alkynyl)gold(I) anionic dimer $[\mathbf{8Au}]^-$.

We analyzed different acetone-*d*₆ solutions containing an equimolar mixture of two receptors and the TBACl salt using ¹H NMR spectroscopy. At 213 K, the chemical exchange between the free and bound receptors was slow on the chemical shift timescale. This permitted the observation of separate proton signals for the free and bound receptors, especially in the aromatic region of the ¹H NMR spectra. In this region we observed multiple sets of doublets. Moreover, some of the doublets assigned to different species were overlapped. Nevertheless, the careful and detailed analyses of the ¹H NMR spectra allowed the quantification of the concentrations of the different species involved in the equilibria. We used the integral values to determine relative concentrations and derive the ratio of the complexes' binding constants (see Supplementary Material). We calculated two binding constant ratios by performing direct pairwise competitive experiments: $\text{K}(\mathbf{3} \bullet \text{Cl}^-)/\text{K}(\mathbf{2} \bullet \text{Cl}^-)$ and $\text{K}(\mathbf{2Au} \bullet \text{Cl}^-)/\text{K}(\mathbf{2} \bullet \text{Cl}^-)$. The obtained values were used to derive the $\text{K}(\mathbf{3} \bullet \text{Cl}^-)/\text{K}(\mathbf{2Au} \bullet \text{Cl}^-)$ binding constant ratio without having to experimentally perform the direct pairwise competitive experiment which was expected to be complex due to extensive signal overlapping.

The calculated ratios of binding constants using the bis-iodo receptor **3** as reference are listed in Table 3 and compared with those derived from the ITC experiments. The agreement between them was very good for $\text{K}(\mathbf{3} \bullet \text{Cl}^-)/\text{K}(\mathbf{2} \bullet \text{Cl}^-)$ but the $\text{K}(\mathbf{3} \bullet \text{Cl}^-)/\text{K}(\mathbf{2Au} \bullet \text{Cl}^-)$ ratio

determined by ITC and pair-wise competitive experiments was slightly different. This suggested that the effect caused by the reaction of $2\mathbf{Au} \rightarrow [\mathbf{8Au}]^-$ during the determination of the binding constants using ITC experiments is not completely negligible. In any case, the obtained results supported the previous findings. In dichloromethane and acetone solution, the substitution of one iodo group at the upper rim of “two wall” calix[4]pyrrole $\mathbf{3}$ by an ethynyl-gold(I)PTA unit in $2\mathbf{Au}$ produced a destabilizing effect of the 1:1 complex with chloride that can be quantified in 0.6–0.7 Kcal/mol. The existence of stronger repulsive chloride–pi interactions in the $2\mathbf{Au} \bullet \text{Cl}^-$ compared to the $2 \bullet \text{Cl}^-$ counterparts is supported by ESP calculations. However, the observed drop in binding energy cannot be exclusively ascribed to electrostatic factors. This is because the comparison of the binding energies of complexes $3 \bullet \text{Cl}^-$ ($R = R' = \text{I}$) and $2 \bullet \text{Cl}^-$ ($R = \text{I}$; $R = \text{ethynyl}$) assigned an energetic advantage around -0.4 Kcal/mol to the former (~ -0.5 Kcal/mol in dichloromethane- d_2 and ~ -0.3 Kcal/mol in acetone- d_6). In this case, however, the change in ESP value produced by the modification of the upper rim substituent is small. Here, we are forced to consider solvation effects as the main responsible for the differences observed in binding. We already noticed important solvation/desolvation effects in the anion binding of other “two wall” aryl-extended calix[4]pyrrole in polar solvents reflecting that the entropic term was mainly responsible for the measured free energy differences [20].

Table 3. Values of the binding constants’ ratios determined using the results of ITC experiments and pairwise-competitive binding experiments.

	$K(3 \bullet \text{Cl}^-)/K(n \bullet \text{Cl}^-)^a$	$K(3 \bullet \text{Cl}^-)/K(n \bullet \text{Cl}^-)^b$
Bis-iodo $\mathbf{3}$	1.00	1.00
Mono-iodo-mono-ethynyl $\mathbf{2}$	1.6 ± 0.1	1.4
Mono-nuclear $2\mathbf{Au}$	2.7 ± 0.1	3.8

^a ITC experiments. ^b Pair-wise competitive experiments.

2.6. Theoretical Calculations

In order to gain some insights on the structures of the chloride complexes formed by the “two wall” calix[4]pyrrole receptors, as well as its electronic binding energies, we decided to undertake DFT calculations. Calculations, including geometry optimization, were performed in the gas phase using Turbomole [30,31] at the RI [32–34]-BP86 [35]-D3BJ [36,37]-def2-TZVP [38] (C, H, N, P, O, Au)(def2-ECP(Au)) level of theory. We derived theoretical binding energies based on a 1:1 binding equilibrium (Figure 5).

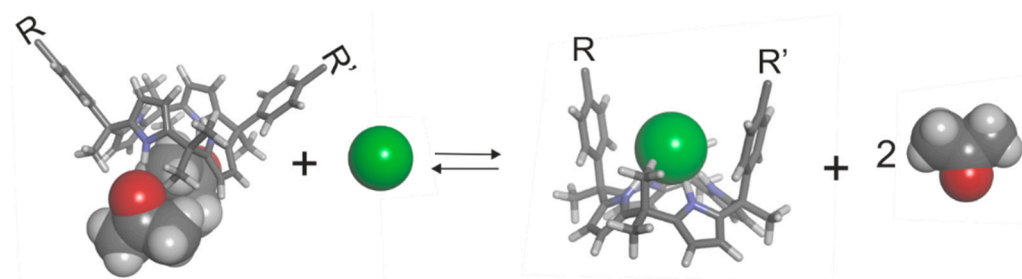


Figure 5. Molecular structures of the species involved in the 1:1 binding equilibrium used to calculate the electronic interaction energies of chloride binding to the receptors’ series: $\Delta E = [E(\text{chloride_complex}) + 2 \times E(\text{acetone})] - [E(\text{acetone solvated 1,3-alternate receptor}) + E(\text{chloride})]$. The receptor is displayed in stick representation. The chloride and the acetone molecules are shown as CPK models.

We evaluated the solvent effect in the binding of chloride by assuming the displacement of two molecules of acetone that originally were bound to the “free” receptor in 1,3-alternate-conformation [39]. The optimized geometry of the 2:1 complexes of acetone with the “free” calix[4]pyrrole displayed one hydrogen-bonding interaction between two

pyrrole NHs and the oxygen atoms of separate acetone molecules. The structure of the acetone solvate was inspired by the solid state structure observed in the X-ray diffraction study of a single crystal of *meso*-hexamethyl-10 α ,20 α -diphenyl calix[4]pyrrole grown from acetone solution [20,40]. The binding of the chloride produced the corresponding 1:1 chloride complex in which the receptor adopted the cone-conformation and two molecules of acetone were released to the bulk solution. The chloride is sandwiched between the *meso*-phenyl substituents and established four convergent hydrogen bonds with the pyrrole NHs.

In the energy minimized structure of the chloride complexes (Figure 6), the distance between the centroid of the *meso*-*p*-iodophenyl ring and the chloride anion decreased from 4.021 Å in the **3**•Cl[−] complex to 3.961 Å in the **2Au**•Cl[−] analogue. Conversely, the distance between the chloride and the differently substituted phenyl ring changed from 4.018 Å for R' = I, 4.040 Å for R' = ethynyl, and 4.076 Å when R' = ethynyl-gold(I)PTA. These results indicated that at the used level of theory, the repulsive nature of the chloride– π interactions can be deduced from the latter geometrical parameter.

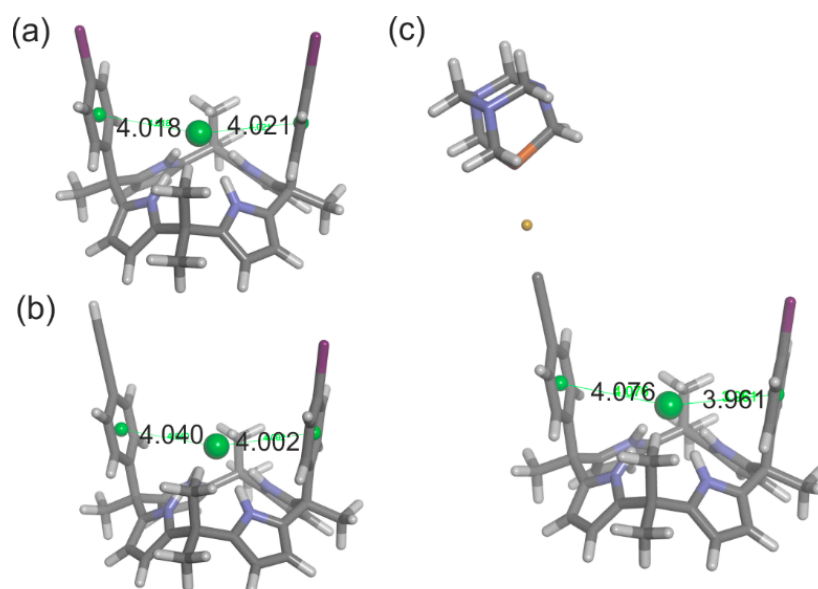


Figure 6. Energy minimized structures at the DFT level of theory of the chloride complexes of the receptor series: (a) **3**•Cl[−]; (b) **2**•Cl[−]; (c) **2Au**•Cl[−]. The distances between the chloride anion and the centroids of the two aromatic rings are shown in Å. The receptors are depicted in stick representation and the chloride as scaled ball.

The magnitudes of the calculated electronic interaction energies are enormous (Table 4). Most likely, this is due to theoretical equilibrium used to estimate them and that the used energies for the species were calculated in the gas phase. Nevertheless, the obtained data reproduced the trend observed in the experimentally measured free energies and binding enthalpies. Using the Cl[−]•**3** complex as reference, the differences between the calculated electronic energies of the complex are of the same order than the experimentally measured differences for their free energies of binding. It is worth noting that the consideration of other equilibria to compute the electronic energies of the complexes i.e., reorganization of one or two solvent molecules from the free receptor to the complex, and/or the use of implicit solvation models produced a larger discrepancy with respect to the experimental results. The obtained results show the importance of adequately modeling the solvent effect in calculations trying to reproduce the trend of experimentally determined free energies of binding in solution and the difficulties of doing it using calculations at the DFT level.

Table 4. Theoretically calculated binding energies for the chloride complexes of the series of “two wall” calix[4]pyrrole receptors.

Complex (n•Cl [−])	ΔE in kcal/mol	ΔΔE in kcal/mol
n = Bis-iodo 3	−32.8502	0
n = Mono-iodo-mono-ethynyl 2	−32.5431	0.3
n = Mono-nuclear 2Au	−31.8133	1.0

2.7. Studies of the Cytotoxicity of **2Au** and the Reference Compound **6Au** Using Human Cancer Cell Lines

Organo-gold and gold coordination-based complexes (e.g., stabilized by NHC, phosphine ligands, etc.) have been described to show cytotoxic activity [41,42]. Specially, alkynyl gold complexes with strong Au–C bonds have been found as promising anticancer drugs [43,44]. We became interested in testing **2Au** for its cytotoxicity towards different human cancer cell lines (HeLa, MIA PaCa-2, and A549) using a cell viability assay based on tetrazolium reduction. We also tested the reference compound **6Au** in order to identify the role played by the calix[4]pyrrole unit in the cytotoxic activity of **2Au**. As summarized in Table 5, the IC₅₀ values determined from the assays of **2Au** in the three cell lines are very similar. We observed an increase in the cytotoxic activity of **2Au** with MIA PaCa-2 cell line. Moreover, **2Au** shows only small differences in activity in A549 cell line compared to the reference compound **6Au**. This result suggested that the calix[4]pyrrole unit does not have a significant effect in the cytotoxic activity of **2Au**. However, we cannot exclude that the presence of the calix[4]pyrrole scaffold endows **2Au** with different properties leading to a different cellular uptake, interaction with biological targets and/or different cell death mechanisms compared to the reference compound **6Au**.

Table 5. IC₅₀ (μM) of **2Au** and **6Au** with HeLa, A549, and MIA PaCa-2 cell lines after 72h of incubation.

Cell Line	IC ₅₀ 2Au (μM)	IC ₅₀ 6Au (μM)
MIA PaCa-2	0.78 ± 0.15	-
A549	0.90 ± 0.26	2.69 ± 0.19
HeLa	1.09 ± 0.71	-

3. Materials and Methods

Reagents were obtained from commercial suppliers and used without further purification unless otherwise stated. All solvents were commercially obtained and used without further purification except pyrrole which was distilled and freshly used. Dry solvents were taken from a solvent system MB SPS 800. Et₃N was dried, distilled and degassed by three freeze-pump-thaw cycles before used in the cross-coupling reactions. Routine ¹H NMR and ¹³C(¹H) NMR spectra were recorded on a Bruker Avance 300 (300 MHz for ¹H NMR and 75 MHz for ¹³C NMR), Bruker Avance 400 (400 MHz for ¹H NMR and 100 MHz for ¹³C NMR), Bruker Avance 500 (500 MHz for ¹H NMR and 125 MHz for ¹³C NMR), or Bruker Avance 500 with cryoprobe (500 MHz for ¹H NMR and 125 MHz for ¹³C NMR). Deuterated solvents used are indicated in the characterization and chemical shifts are given in ppm. Residual solvent peaks were used as reference [45]. All NMR *J* values are given in Hz. COSY, NOESY, HMQC, and HMBC experiments were recorded to help with the assignment of ¹H and ¹³C signals. High Resolution Mass Spectra (HRMS) were obtained on a Bruker HPLC-TOF (MicroTOF Focus), Bruker Corporation, Bremen, Germany, with ESI as ionization mode and Bruker HPLC-QqTOF (MaXis Impact), Bruker Corporation, Bremen, Germany with ESI as ionization mode. Nominal mass spectra were obtained by direct injection on an Agilent 1200 and as detection unit an Agilent 6130 quadrupole. IR spectra were recorded on a Bruker Optics FTIR Alpha spectrometer equipped with a DTGS detector, KBr beamsplitter at 4 cm^{−1} resolution using a one bounce ATR accessory with diamond windows. Melting points were measured on a MP70 Melting Point System Mettler Toledo. Column chromatography was performed with silica gel technical grade (Sigma-Aldrich,

Merck Life Science S. L. U., Madrid, Spain), pore size 60 Å, 230–400 mesh particle size, 40–63 µm particle size and Thin Layer Chromatography (TLC) analysis on silica gel 60 F254. ITC experiments were performed using a MicroCal VP-ITC MicroCalorimeter with the VP Viewer 2000 software, Microcal, version 7.0, Northampton, MA, USA.

3.1. ^1H NMR Titration Experiments

A solution of host (2–5 mM), **3**, **2**, or **2Au**, was prepared in dichloromethane- d_2 or acetone- d_6 . Subsequently, 0.5 mL of the solution were transferred to an NMR tube. The remaining solution of the host was used to prepare the titrant's solution, which contained TBACl at 20-fold higher concentration ($[\text{TBACl}] = 40 \text{ mM}$ and $[\text{H}] = 2\text{--}5 \text{ mM}$). In this manner, the concentration of the host was maintained constant throughout the titration. Immediately, the 0.5 mL of the host solution was titrated by manually injecting incremental amounts of the titrant's solution using a micro syringe. A ^1H NMR spectrum of the mixture was acquired after each injection and vigorous hand shaking of the NMR tube for few seconds. The apparent binding constants were derived from the fit of the chemical shift changes of the titration data to a 1:1 theoretical binding model and using the HypNMR2008 [24,25] software., Hyperquad, version 4.0.66, Leeds, England, UK, <http://www.hyperquad.co.uk/>.

3.2. ITC Experiments

All titrations were performed by injecting small aliquots (8 µL, 16 s) of acetone solution of the TBACl from a computer controlled micro syringe into the solution of the hosts (**3**, **2**, and **2Au**, 0.6–0.8 mM) in the same solvent placed in the cell. The concentration of the TBACl solutions were approximately ten times more concentrated than the receptor ones (6.5–7.7 mM). The temperature was set to 288 K. The apparent association constants and enthalpy values were derived from the fit of the titration data to a 1:1 binding model implemented in the Microcal ITC Data Analysis module.

3.3. Pair-Wise NMR Competitive Experiments

A series of pair-wise NMR competitive titration experiments were performed using receptors **3**, **2**, and **2Au** (receptors A, B, and C), and the TBACl (guest G) in acetone- d_6 . Stock solutions of the receptors in acetone- d_6 were prepared. Equimolar 1:1:1 mixtures of two receptors and TBACl were prepared in independent NMR tubes by adding the appropriate amount of each stock solution in acetone- d_6 to reach a final concentration 4–5 mM (final volume: 500 µL). The ^1H NMR spectra were acquired at 213 K in order to observe separate signals for the bound and free species. The binding constant ratio between the two competing complexes (i.e., AG and BG) was determined by integration of selected proton signals in the acquired ^1H NMR spectra ($K_A/K_B = ([\text{AG}] \times [\text{B}])/([\text{BG}] \times [\text{A}])$).

3.4. Cell Culture

HeLa (human cervical carcinoma), A549 (human lung carcinoma) and MIA PaCa-2 (human pancreatic carcinoma) cells were cultured in high glucose DMEM (Dulbecco's Modified Eagle's Medium) supplemented with 5% fetal bovine serum (FBS), penicillin 200 U mL $^{-1}$, streptomycin 100 µg mL $^{-1}$ and (L)-glutamine 2 mM. Cultures were stored in a humid atmosphere with 95% air/5% CO $_2$ at 37 °C. Cultures were maintained at 37 °C in a humidified atmosphere of 95% air/5% CO $_2$.

3.5. Cytotoxic Assay

The MTT assay was used to determine cell viability as an indicator of cell sensitivity to the compounds. Exponentially growing cells were seeded at a density of approximately 104 cells per well (HeLa and A549) or 105 cells mL $^{-1}$ (MIA-PaCa-2) in 96-well flat-bottomed microplates and allowed to attach for 24 h before the addition of compounds. The compounds were dissolved in DMSO and added to cells in concentrations ranging from 0.25 to 100 µM in quadruplicate. Cells were incubated with the tested compounds for 72 h at 37 °C.

A total of 10 μL of MTT (5 mg mL^{-1}) was added to each well and plates were incubated for 2 h at 37°C . Finally, media was eliminated and DMSO ($100 \mu\text{L}$ per well) was added to dissolve the formed precipitate. The optical density was measured at 550 nm using a 96-well multi scanner auto reader (ELISA). The IC_{50} was calculated by nonlinear regression analysis using the OriginPro 2021 software, OriginLab Corporation, Northampton, MA, USA, <https://www.originlab.com/>. Each compound was analyzed at least in three independent experiments.

4. Conclusions

We report the synthesis of the mono-nuclear organo-gold(I)-PTA “two wall” aryl extended calix[4]pyrrole receptor **2Au**. We performed ^1H NMR titration experiments in dichloromethane- d_2 and acetone- d_6 of **2Au** and their precursors, the mono-iodo mono-ethynyl **2** and the reference bis-iodo **3**, with TBACl. We also performed ITC and pair-wise competitive ^1H NMR experiments in acetone to accurately determine the differences in binding. Taken together, the titration data reveal a ~ 2 - and ~ 3 -fold decrease in the binding constant of mono-iodo mono-ethynyl **2** and mono-nuclear **2Au**, respectively, compared to the reference receptor bis-iodo **3**. The calculated ΔG of the complexes allow us to dissect the binding energies of **2Au** vs. **3** for TBACl into ~ 0.4 kcal/mol produced by the substitution of one iodo substituent by an ethynyl group and ~ 0.3 kcal/mol caused by the incorporation of a gold(I)-PTA moiety in the terminal ethynyl. DFT calculations were also in agreement with the experimental results and nicely reproduced the trend observed in the determined free energy values. However, the differences in the calculated ESP values at the centers of the aromatic ring and at the *para*-substituent of the differently-substituted aromatic walls was not enough to explain the dissimilar free energies of binding of the 1:1 chloride complexes exclusively in terms of repulsive anion- π interactions. Therefore, we conclude that solvation/desolvation processes have a strong contribution to the measured differences.

In agreement with previous findings [12], the addition of more than 1 equiv. of TBACl to a dichloromethane and acetone solution of **2Au** provoked the appearance of two set of aromatic signals for the bound calix[4]pyrrole units. The model compound **6Au**, lacking the calix[4]pyrrole unit, transformed into the gold(I)-anionic dimer $[\mathbf{7Au}]^-$ upon addition of TBACl. This finding led us to conclude that in the titrations of **2Au** with the salt an analogous calix[4]pyrrole gold(I)anionic dimer $[\mathbf{8Au}]^-$ is produced with the concomitant appearance of free PTA and the PTA-Au(I)Cl complex. We assigned the two sets of signals observed for the aromatic protons of the bound calix[4]pyrrole unit in the ^1H NMR spectra of the titrations of **2Au** with TBACl to the formation of the corresponding chloride complexes of **2Au** and $[\mathbf{8Au}]^-$. We also are forced to disregard our previous hypothesis [12] suggesting that the mono-nuclear gold(I) calix[4]pyrrole receptor **1Au** adopted cone and half-cone conformations in the 1:1 complex with chloride. The results of the cytotoxicity studies of **2Au** using different human cancer cell lines assigned IC_{50} values close to $1 \mu\text{M}$. The cytotoxic activity of **2Au** is comparable to that of **6Au** ($2.7 \mu\text{M}$) suggesting that the calix[4]pyrrole moiety has a reduced effect. Nevertheless, we cannot rule out the possibility that the calix[4]pyrrole unit endows the compound with different biological properties (cellular uptake, biological target and cell death mechanisms).

Supplementary Materials: The following supporting information can be downloaded at <https://www.mdpi.com/article/10.3390/inorganics10070095/s1>, Scheme S1. Synthesis of compound **4**; Scheme S2. Synthesis of compound **2**; Scheme S3; Synthesis of compound **2Au**; Scheme S4. Synthesis of $(\text{tht})\text{AuCl}$; Scheme S5. Synthetic scheme for the preparation of the model p-ethynyl-toluene gold(I) complex **6Au**; Scheme S6. Reaction of **6Au** with an excess of TBACl to produce the dimeric anionic species $[\mathbf{7Au}]^-$; Scheme S7. Scheme of the side reaction of the chloride complex of **2Au** with an excess of TBACl to produce chloride complexes of the anionic dimer $[\mathbf{8Au}]^-$. Table S1: Table of induced chemical shifts of the titration of **2Au** with TBACl; Table S2: Table of induced chemical shifts of **2** upon addition of TBACl; Table S3: Table of induced chemical shifts of **3** upon addition of TBACl; Table S4: Binding constants (K) and the thermodynamic parameters (ΔH , $\Delta\text{T}\Delta\text{S}$ and ΔG in $\text{Kcal}\cdot\text{mol}^{-1}$) obtained from the ITC titration experiments of TBACl and **2**, **3** and **2Au** at 288 K in

acetone. Figures S1–S6: NMR characterization of compound **4**. Figures S7–S13: NMR characterization of compound **2**. Figures S14–S18: NMR characterization of compound **2Au**; Figures S19–S21: NMR characterization of compound **6Au**; Figures S22–S25: ^1H NMR titrations of **2Au** with TBACl in DCM: spectra and fit of the chemical shifts; Figures S26–S29: ^1H NMR titrations of **2** with TBACl in DCM: spectra and fit of the chemical shifts; Figures S30–S33: ^1H NMR titrations of **3** with TBACl in DCM: spectra and fit of the chemical shifts; Figures S34 and S35: ^1H NMR titrations of **2** and **3** with TBACl in acetone; Figure S36–S38: Isothermal Titration Calorimetry experiments in acetone. Figure S39: Thermodynamic parameters (ΔH , $T\Delta S$ and ΔG in $\text{Kcal}\cdot\text{mol}^{-1}$) of the 1:1 complexes of **2Au**, **2** and **3** with TBACl in acetone; Figures S40–S46: NMR experiments from the study of the formation of the anionic-bis(alkynyl)gold(I) complexes [**7Au**] $^-$ and [**8Au**] $^-$; Figures S47–S50: ^1H NMR Pair-wise competitive experiments.

Author Contributions: Conceptualization, P.B.; methodology, A.R.; formal analysis, P.B. and M.C.G.; writing—original draft preparation, P.B. and A.R.; writing—review and editing, P.B., G.A., and M.C.G.; supervision, P.B. All authors have read and agreed to the published version of the manuscript.

Funding: This research was funded by Gobierno de España MICINN/AEI/FEDER, UE (PID2020-114020GB-I00 and CEX2019-000925-S), the CERCA Programme/Generalitat de Catalunya, and AGAUR (2017 SGR 1123). A.R. thanks MICINN for a predoctoral fellowship (FPI-PRE-2018-086087).

Conflicts of Interest: The authors declare no conflict of interest.

References and Notes

- Herrera, R.P.; Gimeno, M.C. Main Avenues in Gold Coordination Chemistry. *Chem. Rev.* **2021**, *121*, 8311–8363. [[CrossRef](#)] [[PubMed](#)]
- Gil-Rubio, J.; Vicente, J. The Coordination and Supramolecular Chemistry of Gold Metalloligands. *Chem. Eur. J.* **2018**, *24*, 32–46. [[CrossRef](#)]
- Hau, F.K.-W.; Yam, V.W.-W. Synthesis and cation-binding studies of gold(i) complexes bearing oligoether isocyanide ligands with ester and amide as linkers. *Dalton Trans.* **2016**, *45*, 300–306. [[CrossRef](#)] [[PubMed](#)]
- He, X.; Lam, W.H.; Zhu, N.; Yam, V.W.-W. Design and Synthesis of Calixarene-Based Bis-alkynyl-Bridged Dinuclear AuI Isonitrile Complexes as Luminescent Ion Probes by the Modulation of Au...Au Interactions. *Chem. Eur. J.* **2009**, *15*, 8842–8851. [[CrossRef](#)] [[PubMed](#)]
- Yam, V.W.-W.; Cheung, K.-L.; Yuan, L.-H.; Wong, K.M.-C.; Cheung, K.-K. Synthesis, structural characterization and binding studies of a novel dinuclear gold(i) calix[4]crown acetylide complex. *Chem. Commun.* **2000**, 1513–1514. [[CrossRef](#)]
- Zhou, Y.-P.; Zhang, M.; Li, Y.-H.; Guan, Q.-R.; Wang, F.; Lin, Z.-J.; Lam, C.-K.; Feng, X.-L.; Chao, H.-Y. Mononuclear Gold(I) Acetylide Complexes with Urea Group: Synthesis, Characterization, Photophysics, and Anion Sensing Properties. *Inorg. Chem.* **2012**, *51*, 5099–5109. [[CrossRef](#)] [[PubMed](#)]
- Shi, H.-Y.; Qi, J.; Zhao, Z.-Z.; Feng, W.-J.; Li, Y.-H.; Sun, L.; Lin, Z.-J.; Chao, H.-Y. Synthesis, characterization, photophysics, and anion binding properties of gold(i) acetylide complexes with amide groups. *New J. Chem.* **2014**, *38*, 6168–6175. [[CrossRef](#)]
- Gale, P.A.; Sessler, J.L.; Král, V.; Lynch, V. Calix[4]pyrroles: Old Yet New Anion-Binding Agents. *J. Am. Chem. Soc.* **1996**, *118*, 5140–5141. [[CrossRef](#)]
- Rather, I.A.; Wagay, S.A.; Hasnain, M.S.; Ali, R. New dimensions in calix[4]pyrrole: The land of opportunity in supramolecular chemistry. *RSC Adv.* **2019**, *9*, 38309–38344. [[CrossRef](#)]
- Kim, S.K.; Sessler, J.L. Calix[4]pyrrole-Based Ion Pair Receptors. *Acc. Chem. Res.* **2014**, *47*, 2525–2536. [[CrossRef](#)]
- Cafeo, G.; Carbotti, G.; Cuzzola, A.; Fabbi, M.; Ferrini, S.; Kohnke, F.H.; Papanikolaou, G.; Plutino, M.R.; Rosano, C.; White, A.J.P. Drug Delivery with a Calixpyrrole–trans-Pt(II) Complex. *J. Am. Chem. Soc.* **2013**, *135*, 2544–2551. [[CrossRef](#)] [[PubMed](#)]
- Sun, Q.; Aragay, G.; Pinto, A.; Aguiló, E.; Rodríguez, L.; Ballester, P. Influence of the Attachment of a Gold(I) Phosphine Moiety at the Upper Rim of a Calix[4]pyrrole on the Binding of Tetraalkylammonium Chloride Salts. *Chem. Eur. J.* **2020**, *26*, 3348–3357. [[CrossRef](#)] [[PubMed](#)]
- Wu, Y.-D.; Wang, D.-F.; Sessler, J.L. Conformational Features and Anion-Binding Properties of Calix[4]pyrrole: A Theoretical Study. *J. Org. Chem.* **2001**, *66*, 3739–3746. [[CrossRef](#)] [[PubMed](#)]
- Blas, J.R.; López-Bes, J.M.; Márquez, M.; Sessler, J.L.; Luque, F.J.; Orozco, M. Exploring the Dynamics of Calix[4]pyrrole: Effect of Solvent and Fluorine Substitution. *Chem. Eur. J.* **2007**, *13*, 1108–1116. [[CrossRef](#)]
- Valderrey, V.; Escudero-Adán, E.C.; Ballester, P. Polyatomic Anion Assistance in the Assembly of [2]Pseudorotaxanes. *J. Am. Chem. Soc.* **2012**, *134*, 10733–10736. [[CrossRef](#)]
- Valderrey, V.; Escudero-Adán, E.C.; Ballester, P. Highly Cooperative Binding of Ion-Pair Dimers and Ion Quartets by a Bis(calix[4]pyrrole) Macrotricyclic Receptor. *Angew. Chem. Int. Ed.* **2013**, *52*, 6898–6902. [[CrossRef](#)]
- Kemper, B.; Hristova, Y.R.; Tacke, S.; Stegemann, L.; van Bezouwen, L.S.; Stuart, M.C.A.; Klingauf, J.; Strassert, C.A.; Besenius, P. Facile synthesis of a peptidic Au(i)-metalloamphiphile and its self-assembly into luminescent micelles in water. *Chem. Commun.* **2015**, *51*, 5253–5256. [[CrossRef](#)]

18. Aguiló, E.; Gavara, R.; Baucells, C.; Guitart, M.; Lima, J.C.; Llorca, J.; Rodríguez, L. Tuning supramolecular aurophilic structures: The effect of counterion, positive charge and solvent. *Dalton Trans.* **2016**, *45*, 7328–7339. [[CrossRef](#)]
19. McArdle, C.P.; Van, S.; Jennings, M.C.; Puddephatt, R.J. Gold(I) Macrocycles and Topologically Chiral [2]Catenanes. *J. Am. Chem. Soc.* **2002**, *124*, 3959–3965. [[CrossRef](#)]
20. Adriaenssens, L.; Gil-Ramírez, G.; Frontera, A.; Quiñonero, D.; Escudero-Adán, E.C.; Ballester, P. Thermodynamic Characterization of Halide– π Interactions in Solution Using “Two-Wall” Aryl Extended Calix[4]pyrroles as Model System. *J. Am. Chem. Soc.* **2014**, *136*, 3208–3218. [[CrossRef](#)]
21. Kim, S.K.; Sessler, J.L. Ion pair receptors. *Chem. Soc. Rev.* **2010**, *39*, 3784–3809. [[CrossRef](#)] [[PubMed](#)]
22. Ciardi, M.; Tancini, F.; Gil-Ramírez, G.; Escudero Adán, E.C.; Massera, C.; Dalcanale, E.; Ballester, P. Switching from Separated to Contact Ion-Pair Binding Modes with Diastereomeric Calix[4]pyrrole Bis-phosphonate Receptors. *J. Am. Chem. Soc.* **2012**, *134*, 13121–13132. [[CrossRef](#)] [[PubMed](#)]
23. The second set of proton signal showing a reduced intensity were not considered for the fit.
24. Frassinetti, C.; Ghelli, S.; Gans, P.; Sabatini, A.; Moruzzi, M.S.; Vacca, A. Nuclear Magnetic Resonance as a Tool for Determining Protonation Constants of Natural Polyprotic Bases in Solution. *Anal. Biochem.* **1995**, *231*, 374–382. [[CrossRef](#)] [[PubMed](#)]
25. Frassinetti, C.; Alderighi, L.; Gans, P.; Sabatini, A.; Vacca, A.; Ghelli, S. Determination of protonation constants of some fluorinated polyamines by means of ^{13}C NMR data processed by the new computer program HypNMR2000. Protonation sequence in polyamines. *Anal. Bioanal. Chem.* **2003**, *376*, 1041–1052.
26. Abu-salah, O.M. A Novel Method for the Preparation of Two bis(arylethynyl)-aurate(I) Complex Anions. *J. Chem. Res. Synop.* **1984**, *187*. Available online: <http://pascal-francis.inist.fr/vibad/index.php?action=getRecordDetail&idt=9579027> (accessed on 1 July 2022).
27. Vicente, J.; Chicote, M.-T.; Alvarez-Falcon, M.M.; Jones, P.G. Gold(I) Complexes Derived from $\text{C}_6\text{Me}_3(\text{C}\equiv\text{CH})_3$ -1,3,5, $\text{C}_6\text{Me}_4(\text{C}\equiv\text{CH})_2$ -1,4, and $\text{MeC}_6\text{H}_4\text{C}\equiv\text{CH}$ -4. *Organometallics* **2005**, *24*, 5956–5963. [[CrossRef](#)]
28. Liu, Q.; Xie, M.; Chang, X.; Cao, S.; Zou, C.; Fu, W.-F.; Che, C.-M.; Chen, Y.; Lu, W. Tunable Multicolor Phosphorescence of Crystalline Polymeric Complex Salts with Metallophilic Backbones. *Angew. Chem. Int. Ed.* **2018**, *57*, 6279–6283. [[CrossRef](#)]
29. Abu-Salah, O.M.; Al-Ohaly, A.R.A.; Al-Showiman, S.S.; Al-Najjar, I.M. A ^{13}C nuclear magnetic resonance study of some linear alkynyl gold(I) and silver(I) complexes. *Transit. Met. Chem. (Lond.)* **1985**, *10*, 207–210. [[CrossRef](#)]
30. TURBOMOLE V7.0 2015, a Development of University of Karlsruhe and Forschungszentrum Karlsruhe GmbH, 1989–2007, TURBOMOLE GmbH, Since 2007. Available online: <http://www.turbomole.com> (accessed on 1 July 2022).
31. Ahlrichs, R.; Bär, M.; Häser, M.; Horn, H.; Kölmel, C. Electronic structure calculations on workstation computers: The program system turbomole. *Chem. Phys. Lett.* **1989**, *162*, 165–169. [[CrossRef](#)]
32. Eichkorn, K.; Treutler, O.; Ohm, H.; Haser, M.; Ahlrichs, R. Auxiliary Basis-Sets to Approximate Coulomb Potentials (VOL 240, PG 283, 1995). *Chem. Phys. Lett.* **1995**, *242*, 652–660. [[CrossRef](#)]
33. Eichkorn, K.; Weigend, F.; Treutler, O.; Ahlrichs, R. Auxiliary basis sets for main row atoms and transition metals and their use to approximate Coulomb potentials. *Theor. Chem. Acc.* **1997**, *97*, 119–124. [[CrossRef](#)]
34. Sierka, M.; Hogeckamp, A.; Ahlrichs, R. Fast evaluation of the Coulomb potential for electron densities using multipole accelerated resolution of identity approximation. *J. Chem. Phys.* **2003**, *118*, 9136–9148. [[CrossRef](#)]
35. Perdew, J.P. Density-functional approximation for the correlation energy of the inhomogeneous electron gas. *Phys. Rev. B* **1986**, *33*, 8822–8824. [[CrossRef](#)]
36. Grimme, S.; Antony, J.; Ehrlich, S.; Krieg, H. A consistent and accurate ab initio parametrization of density functional dispersion correction (DFT-D) for the 94 elements H-Pu. *J. Chem. Phys.* **2010**, *132*, 154104. [[CrossRef](#)] [[PubMed](#)]
37. Grimme, S.; Ehrlich, S.; Goerigk, L. Effect of the Damping Function in Dispersion Corrected Density Functional Theory. *J. Comput. Chem.* **2011**, *32*, 1456–1465. [[CrossRef](#)] [[PubMed](#)]
38. Weigend, F.; Ahlrichs, R. Balanced basis sets of split valence, triple zeta valence and quadruple zeta valence quality for H to Rn: Design and assessment of accuracy. *Phys. Chem. Chem. Phys.* **2005**, *7*, 3297–3305. [[CrossRef](#)]
39. Other considerations of the theoretical equilibrium i.e., Use of implicit solvation or explicit solvation of the complexes with one or two molecules of acetone produced results that were in contrast with the experimental ones.
40. CCDC 1002710 Contains the Crystallographic Data. Refcode: BOGWIF. Available online: <https://www.ccdc.cam.ac.uk/> (accessed on 1 July 2022).
41. Montanel-Pérez, S.; Elizalde, R.; Laguna, A.; Villacampa, M.D.; Gimeno, M.C. Synthesis of Bioactive N-Acyclic Gold(I) and Gold(III) Diamino Carbenes with Different Ancillary Ligands. *Eur. J. Inorg. Chem.* **2019**, *2019*, 4273–4281. [[CrossRef](#)]
42. Quero, J.; Ruighi, F.; Osada, J.; Gimeno, M.C.; Cerrada, E.; Rodríguez-Yoldi, M.J. Gold(I) Complexes Bearing Alkylated 1,3,5-Triaza-7-phosphaadamantane Ligands as Thermoresponsive Anticancer Agents in Human Colon Cells. *Biomedicines* **2021**, *9*, 1848. [[CrossRef](#)]
43. Cerrada, E.; Fernández Moreira, V.; Gimeno, M.C. Chapter 4: Gold and Platinum Alkynyl Complexes for Biomedical Applications in *Advances in Organometallic Chemistry*; Pérez, P.J., Ed.; Academic Press: Cambridge, MA, USA, 2019; Volume 71, pp. 227–258.
44. Yang, Z.; Jiang, G.; Xu, Z.; Zhao, S.; Liu, W. Advances in alkynyl gold complexes for use as potential anticancer agents. *Coord. Chem. Rev.* **2020**, *423*, 213492. [[CrossRef](#)]
45. Fulmer, G.R.; Miller, A.J.M.; Sherden, N.H.; Gottlieb, H.E.; Nudelman, A.; Stoltz, B.M.; Bercaw, J.E.; Goldberg, K.I. NMR Chemical Shifts of Trace Impurities: Common Laboratory Solvents, Organics, and Gases in Deuterated Solvents Relevant to the Organometallic Chemist. *Organometallics* **2010**, *29*, 2176–2179. [[CrossRef](#)]